

Tritium Retention in Hexavalent Chromate-Conversion-Coated Aluminum Alloy

Introduction

Aluminum is used as a material for the OMEGA target chamber walls and for diagnostics that are in close proximity to the target chamber because of the small number of impurities contained in the lattice and the short lifetime of any neutron-activated isotopes. This material selection mitigates the radiological factors that stem from DT neutron activation but does not account for tritium interactions with the metal. It is well established that tritium will migrate from the gas phase into the metal bulk. Previous work has shown that surface modifications of materials have a tremendous impact on the total quantity of tritium retained by the sample.¹⁻⁴

Hexavalent chromium-conversion coatings increase the corrosion resistance of aluminum alloy by forming a layer of Cr(III) hydroxide.^{5,6} This passive layer can increase the lifetime of the aluminum piece by inhibiting corrosion. The mechanism of chromate-conversion coating (CCC) on an aluminum alloy is proposed to proceed by a sol-gel route.^{5,7} In the sol-gel mechanism, a coupled redox reaction occurs that oxidizes aluminum metal and activates the hexavalent chromium-coating material by reducing the chromium. The aqueous solution containing both trivalent chromium and trivalent aluminum species will further react through hydrolysis to form a network of chromium hydride as shown in Fig. 155.10.

Upon drying, these polymeric hydrated films of chromium hydroxide collapse to form a cracked, broken network of chromium hydroxide on the surface of the material. These chromium layers act as a barrier to corrosion of the underlying aluminum substrate; however, there have been no studies to investigate how these films interact with a tritium environment.

Experimental Setups and Procedures

Samples of dimensions $5.1 \times 1.9 \times 0.3 \text{ cm}^3$ were cut from a common plate of aluminum 6061. Approximately 0.86 mm of the surface was machined away to eliminate any surface inclusions that can arise from manufacturing. Samples that did not receive any further surface modifications were degreased first with acetone, followed by water, and finally isopropyl alcohol to dry the samples; these samples are referred to as “unmodified.” Conversely, a set of samples had the surface modified by the commercial CCC described above. Materials characterization was performed to understand the chemical and microstructure of the unmodified and CCC films.

An x-ray photoelectron spectroscopy (XPS) analysis of the CCC films on aluminum supports the sol-gel formation of chromium hydroxide on the surface. All spectra were recorded after a 10-min argon-ion gun etch (5 keV) to remove any adven-

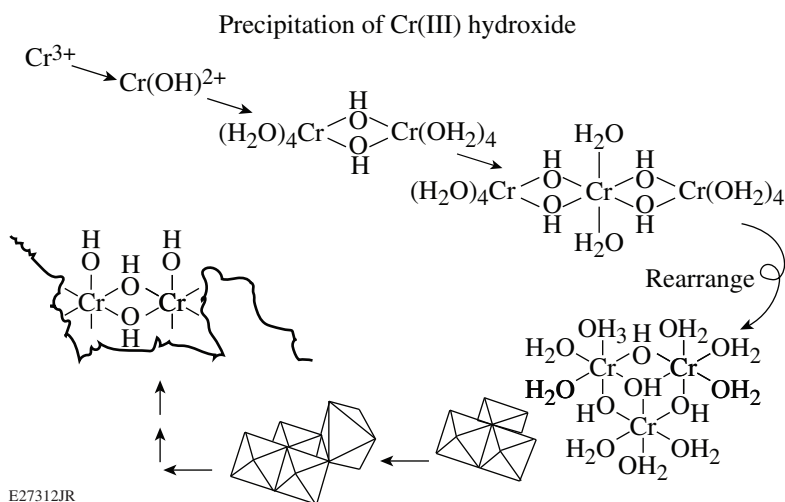
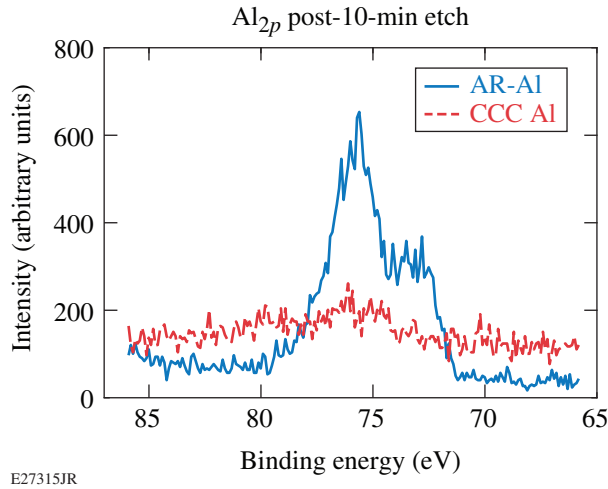


Figure 155.10
Schematic representation of chromium hydroxide [Cr(III)] precipitation and subsequent binding to the target substrate. (Reprinted with permission from The Electrochemical Society.⁷)

E27312JR

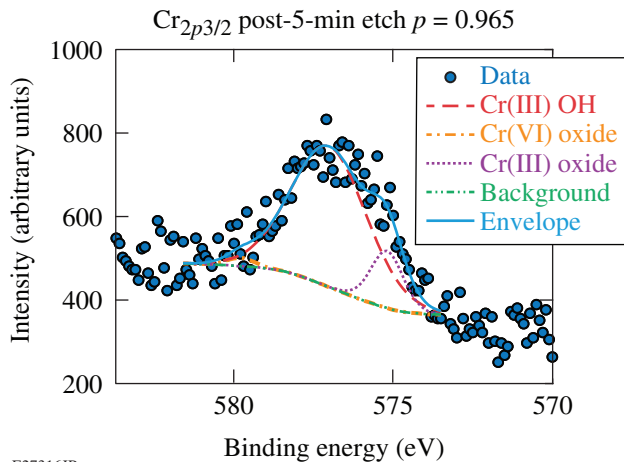
titious carbon species on the surface. Figure 155.11 shows the Al_{2p} spectrum for both the unmodified aluminum and the CCC aluminum samples. The data suggest that complete coverage was achieved on the CCC films, indicated by the lack of aluminum binding states present on the surface of the sample. The $Cr_{2p3/2}$ spectrum of the CCC films on aluminum, shown in Fig. 155.12, revealed several chromium species in the layer.



E27315JR

Figure 155.11

X-ray photoelectron spectroscopy (XPS) spectra of unmodified aluminum [Ar-Al] (blue) and chromate-conversion-coating (CCC) [CCC Al] films on aluminum (red). No appreciable amounts of aluminum are present in the CCC films, indicating complete conversion.



E27316JR

Figure 155.12

$Cr_{2p3/2}$ spectrum of the CCC films on aluminum. Raw data (circles) and fits (colored lines) indicate the binding states found on the surfaces. The decomposition of the photoelectron peak indicates several chromium species present on the surface of the CCC aluminum. The p value for the envelope fit was determined to be 0.965.

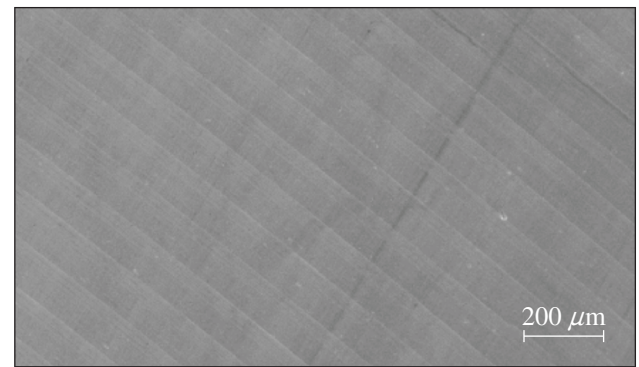
Using the peak fitting software CasaXPS, a fitting routine was used to decompose the $Cr_{2p3/2}$ photoelectron peak. The results of the fitting routine are shown in Table 155.I.

Table 155.I: $Cr_{2p3/2}$ fit results obtained from the fitting routine using CasaXPS.

Species	Area (%)	Mean Energy (eV)
Cr(III) OH	88.7	577.1
Cr(III) oxide	14.5	579.8
Cr(IV) oxide	1.76	575.2

The results of the $Cr_{2p3/2}$ fit also support the sol-gel formation because of the large quantities of chromium hydroxide present in the CCC film along with small amounts of Cr(III) oxide and Cr(VI) oxide.

The CCC film process on aluminum significantly altered the microstructure compared to unmodified samples. The scanning electron microscope (SEM) micrograph for unmodified aluminum is shown in Fig. 155.13. The only extraordinary features stem from the machining process and are apparent at the 200- μ m scale. No smaller features were visible. These films contain large quantities of fractures and cracks likely caused by the collapse of the polymeric network during air drying of the films.



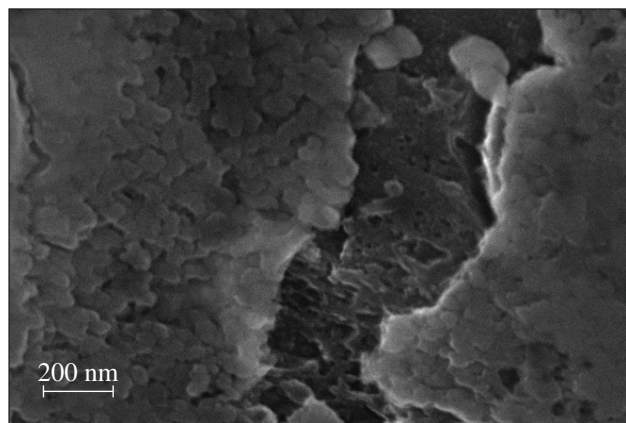
E27708JR

Figure 155.13

Scanning electron microscopy (SEM) micrograph of unmodified aluminum, where machine markings are apparent at the 200- μ m scale with 20-kV accelerating voltage, 17.5-mm working distance, and 23 \times magnification.

A detailed view of the CCC aluminum sample is shown in Fig. 155.14. The highly grained structure is quite apparent at higher magnification. The grain size of the chromium

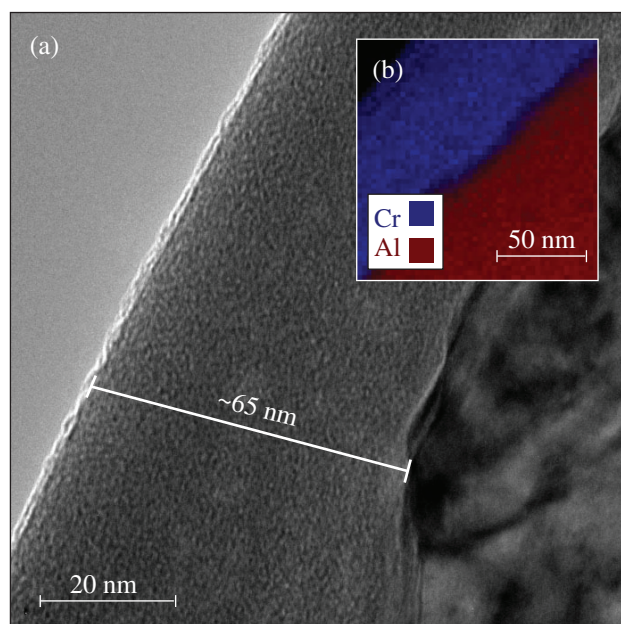
hydroxide is of the order of 50 to 100 nm, while the dislocation fracture is ~ 300 nm. To obtain a better understanding of the microstructure, a cross-section sample was prepared for transmission electron microscopy (TEM) analysis. The results in Fig. 155.15 show that the CCC layer is, on average, 65 nm



E27709JR

Figure 155.14

A detailed view of a pit present in the CCC film on aluminum. The scale bar indicates a 200-nm scale with 20-kV accelerating voltage, 5.8-mm working distance, and 59.13 \times magnification. The highly grained structure of the CCC films on aluminum is apparent at this scale.



E27357JR

Figure 155.15

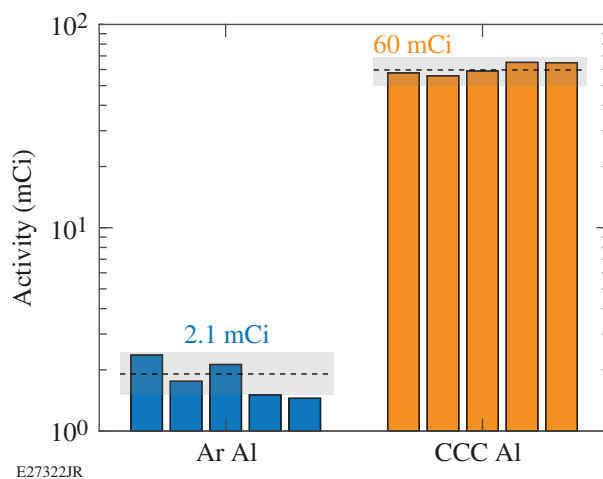
TEM cross section of the CCC film on aluminum on a 20-nm scale. The porous nature can be inferred from highly grained film. Inset: STEM x-ray map of the CCC film, where both chromium (blue) and aluminum (red) species are shown.

thick. This was visually apparent and also confirmed with the scanning transmission electron microscopy (STEM) x-ray map shown in Fig. 155.15.

The chemistry and microstructure of the CCC samples indicate a stark difference between the unmodified and modified aluminum samples; however, the impact these differences have on tritium retention is unconfirmed. To determine the impact, samples were charged with tritium by exposure to a deuterium-tritium (DT) gas mixture at 25°C for 24 h. After exposure, the samples were stored in separate metal containers under a dry helium atmosphere until retrieved for an experiment.

Results and Discussion

The tritium-charged samples were subjected to one of two treatments: thermal desorption or a surface-stripping wash. In the first treatment, samples were subjected to temperature-programmed thermal desorption (TPD) to thermally remove and measure the total quantity of tritium retained by the metal sample. Tritium was collected as tritiated water in bubblers attached to the furnace. The activity was measured by scintillation counting using a PerkinElmer Tri-Carb 2910 TR liquid scintillation counter. The results of the TPD experiments for both the unmodified and CCC samples are shown in Fig. 155.16.



E27322JR

Figure 155.16

Total activity measured with temperature-programmed thermal desorption (TPD) on a semi-log plot. Each bar represents an individual sample; the bars are grouped by surface finish unmodified aluminum (blue) and CCC Al (orange). The mean of each group is shown as a dashed line, with the error plotted between the shaded regions.

The TPD results indicate that, on average, the unmodified aluminum samples retained a total of 2.1 mCi. While the total activity in the aluminum samples was lower than expected, the CCC aluminum retained 60 mCi. This large difference reveals that the CCC samples retained 30× more tritium than the unmodified counterpart. This increase cannot be explained by a purely diffusive argument and most likely stems from the large quantities of hydrated chromium hydroxide and the surface defects observed with XPS and SEM/TEM, respectively.

In the second treatment, samples were washed in 75 mL of a 15% surfactant solution for 5 min. In this solution, tritium on and in the near surface of the metal is expected to be removed from the metal. The activity in the resulting solution was measured using liquid scintillation counting to give the total quantity of surface/near-surface tritium removed during the wash. The results of the surface washes are shown in Fig. 155.17.

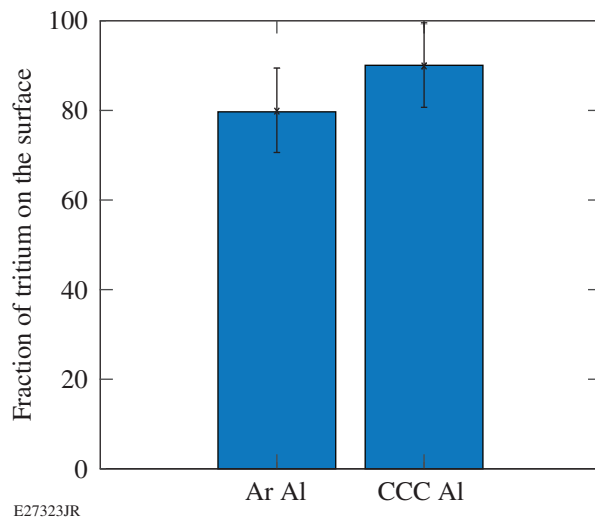


Figure 155.17 The fraction of tritium residing on the surface of the unmodified aluminum (Ar Al) and the CCC aluminum (CCC Al) samples. The resulting surface concentrations of 0.8 Ci/cm³ and 0.4 Ci/cm³ were found for unmodified aluminum and CCC aluminum, respectively.

It was found that >75% of the tritium resides on and in the surface of both unmodified aluminum and CCC aluminum. Taking the total quantity removed in thermal desorption and subtracting the quantity of tritium found on and in the near surface, the partitioning of tritium between the surface and bulk of both unmodified aluminum and the CCC samples is shown in Table 155.II.

Table 155.II: Partitioning of tritium between surface and bulk of unmodified aluminum and CCC aluminum. All values are reported as mCi of tritium.

Sample	Surface	Bulk	Total
Unmodified Al	1.7	0.4	2.1
CCC Al	53	7	60

Under the exposure conditions and using the literature diffusivity of aluminum² at a room temperature of 7.95 × 10⁻¹² m²s⁻¹, an unmodified aluminum sample is expected to reach equilibrium with a tritium inventory of 2.5 mCi. The measured tritium inventory is sevenfold shy of the expected equilibrium value, hinting that the concentration profile in the samples has not reached an equilibrium state. Additionally, for these experimental conditions, the Fourier number (ϕ) suggests that the system is in the transition regime, where a time-dependent analysis is acceptable. The Fourier number is given in Eq. (1), where x is the thickness of the sample, D is the diffusivity, and t is time:

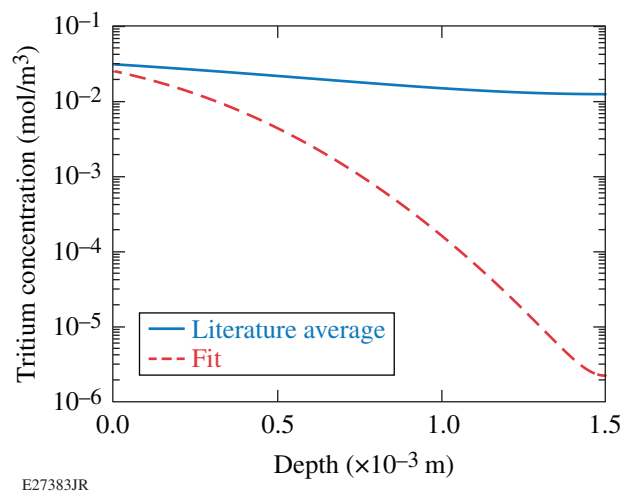
$$\phi = \frac{x^2}{Dt}. \quad (1)$$

Using the literature diffusivity and solubility values,² the concentration profile for the unmodified aluminum samples is obtained from the solution to the semi-infinite diffusion equation.⁸ The concentration profile $c(x,t)$ is given by

$$c(x,t) = c_0 + (c_\infty - c_0) \operatorname{erf}\left(\frac{x}{\sqrt{4Dt}}\right), \quad (2)$$

where c_0 is the solubility (S) in the near surface of the material, D is the diffusivity, and t is the time the diffusion process takes place. This equation was solved using the published values for D and S to yield the blue concentration profile shown in Fig. 155.17. The integral of this profile through the depth of the sample yields 2.5 mCi of total tritium in the bulk.

The concentration profile was also determined using the inventory obtained in the thermal desorption experiment. In this calculation, the $D \times S$ product was varied until the integral of the concentration profile matched the experimental values. The result of this calculation is also shown in Fig. 155.18. The $D \times S$ product for the fit needed to be lowered by a factor of 0.15 to match the measured bulk tritium inventory. It is noteworthy that the modified diffusivity–solubility product for the fit is still within the range of reported literature values.



E27383JR

Figure 155.18

The concentration profiles for the literature D and S values (blue) and the fit values (red) for aluminum 6061 on a double log plot. The $D \times S$ product for the fit was lowered by a factor of 0.15. The integral of the blue and red curves yields 2.5 mCi and 2.1 mCi, respectively.

Conclusions

Chromate-conversion coatings significantly alter the chemistry and microstructure of aluminum alloy by fully converting the aluminum surface to a cracked hydrated chromium hydroxide layer. Also, the CCC films allow for enhanced tritium uptake compared to unmodified aluminum. Most of the tritium retained in the CCC samples resides on the surface, indicating the importance of the surface in the tritium adsorption process and subsequent retention. The high quantities of tritium in all areas of the CCC samples indicated these films are not suited for applications where exposure to tritium is possible.

ACKNOWLEDGMENT

This material is based upon work supported by the Department of Energy National Nuclear Security Administration under Award Number DE-NA0001944, the University of Rochester, and the New York State Energy Research and Development Authority. The support of DOE does not constitute an endorsement by DOE of the views expressed here.

REFERENCES

1. C. Fagan, M. Sharpe, W. T. Shmayda, and W. U. Schröder, *Fusion Sci. Technol.* **71**, 275 (2017).
2. M. Sharpe, W. T. Shmayda, and W. U. Schröder, *Fusion Sci. Technol.* **70**, 97 (2016).
3. T. Hirabayashi, M. Saeki, and E. Tachikawa, *J. Nucl. Mater.* **127**, 187 (1985).
4. R.-D. Penzhorn *et al.*, *Fusion Sci. Technol.* **64**, 45 (2013).
5. J. H. Osborne, *Prog. Org. Coat.* **41**, 280 (2001).
6. P. L. Hagans and C. M. Haas, in *ASM Handbook*, edited by C. M. Cotell, J. A. Sprague, and F. A. Smidt, Jr. (ASM International, Materials Park, OH, 1994), Vol. 5, pp. 405–411.
7. M. W. Kendig and R. G. Buchheit, *Corrosion* **59**, 379 (2003).
8. J. Crank, *The Mathematics of Diffusion* (Oxford University Press, Oxford, 1979).